Randomization and resilience of brain functional networks as systems-level endophenotypes of schizophrenia

Chun-Yi Zac Lo[a], Tsung-Wei Su[b], Chu-Chung Huang[a], Chia-Chun Hung[c,d], Wei-Ling Chen[c], Tsuo-Hung Lan[c], Ching-Po Lin[a,e,1], and Edward T. Bullmore[f,g,h,i]

[a]Institute of Neuroscience, National Yang-Ming University, Taipei 11221, Taiwan; [b]Department of Biomedical Imaging and Radiological Sciences, National Yang-Ming University, Taipei 11221, Taiwan; [c]Department of Psychiatry, Taichung Veterans General Hospital, Taichung 40705, Taiwan; [d]Institute of Brain Science, National Yang-Ming University, Taipei 11221, Taiwan; [e]Brain Research Center, National Yang-Ming University, Taipei 11221, Taiwan; [f]Department of Psychiatry, Behavioural and Clinical Neurosciences Institute, University of Cambridge, Cambridge CB2 0SZ, United Kingdom; [g]Cambridgeshire & Peterborough National Health Service (NHS) Foundation Trust, Cambridge CB21 5EF, United Kingdom; [h]National Institute for Health Research Cambridge Biomedical Research Centre, Cambridge University Hospitals NHS Foundation Trust, Cambridge CB2 0QQ, United Kingdom; and [i]Immunopsychiatry, Alternative Discovery & Development, GlaxoSmithKline, Stevenage SG1 2NY, United Kingdom

Schizophrenia is increasingly conceived as a disorder of brain network organization or dysconnectivity syndrome. Functional MRI (fMRI) networks in schizophrenia have been characterized by abnormally random topology. We tested the hypothesis that network randomization is an endophenotype of schizophrenia and therefore evident also in nonpsychotic relatives of patients. Head movement-corrected, resting-state fMRI data were acquired from 25 patients with schizophrenia, 25 first-degree relatives of patients, and 29 healthy volunteers. Graphs were used to model functional connectivity as a set of edges between regional nodes. We estimated the topological efficiency, clustering, degree distribution, resilience, and connection distance (in millimeters) of each functional network. The schizophrenic group demonstrated significant randomization of global network metrics (reduced clustering, greater efficiency), a shift in the degree distribution to a more homogeneous form (fewer hubs), a shift in the distance distribution (proportionally more long-distance edges), and greater resilience to targeted attack on network hubs. The networks of the relatives also demonstrated abnormal randomization and resilience compared with healthy volunteers, but they were typically less topologically abnormal than the patients' networks and did not have abnormal connection distances. We conclude that schizophrenia is associated with replicable and convergent evidence for functional network randomization, and a similar topological profile was evident also in nonpsychotic relatives, suggesting that this is a systems-level endophenotype or marker of familial risk. We speculate that the greater resilience of brain networks may confer some fitness advantages on nonpsychotic relatives that could explain persistence of this endophenotype in the population.

psychosis | dysconnectivity | graph theory | brain network | hubs

Schizophrenia is increasingly conceived as a brain dysconnectivity syndrome or disorder of brain network organization (1–4). Various methods have been used to demonstrate abnormal structural or functional connectivity between brain regions in patients with schizophrenia. Specifically, several recent studies have used graph theory to measure the topological pattern of connections (or edges) between regional nodes in large-scale networks derived from neuroimaging data (5–12).

The results to date of graph theoretical studies of schizophrenia are not entirely consistent, but there is some convergence around the concept of topological randomization (9, 13). For example, human brain networks (and many other complex, real-life networks) generally have a small-world topology that can be understood as intermediate between the regular, highly clustered organization of a lattice and the globally efficient organization of a random graph. Three independent functional MRI (fMRI) studies have shown that the functional brain networks of patients with schizophrenia are relatively shifted toward the random end of this small-world

spectrum, i.e., they have lower clustering coefficient and greater efficiency than healthy brain networks (5, 7, 8). Previous studies have also reported schizophrenia-related disruptions in the normal community structure of fMRI networks, such as increased connectivity between modules (5), and abnormal rich clubs (14), in patients with schizophrenia. There is also some evidence that the physical (geometric) distance of edges tends to be relatively increased in structural and functional brain graphs of schizophrenia (6, 15).

There were three main objectives of this study. The first was to assess the replicability of the prior topological and geometric markers of network randomization in an independent sample of patients with schizophrenia. Specifically, we wanted to test the hypothesis that the network abnormalities most frequently reported in US or European studies of schizophrenia would also be evident in a Chinese population. Second, we tested the hypothesis that brain network randomization in patients with schizophrenia would be associated with greater resilience to targeted attack on network hubs in silico. Third, we aimed to

Significance

Using network analysis of resting-state functional MRI data, we demonstrate that significant randomization of global network metrics, and greater resilience to targeted attack on network hubs, was replicably demonstrable in Chinese patients with schizophrenia, and was also demonstrated for the first time in their nonpsychotic first-degree relatives. These results support the hypothesis that functional networks are abnormally randomized and resilient in schizophrenia and indicate that network randomization/resilience may be an endophenotype, or marker of familial risk, for schizophrenia. We suggest that the greater randomization of the brain network endophenotype of schizophrenia may confer advantages in terms of greater resilience to pathological attack that may explain the selection and persistence of risk genes for schizophrenia in the general population.
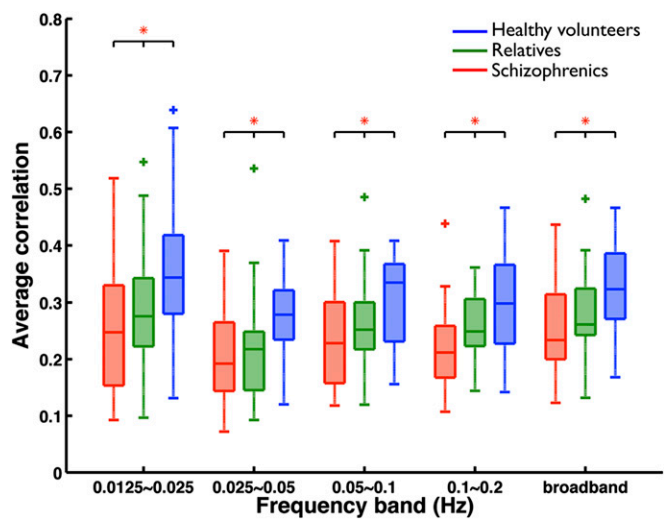
Fig. 1. Global functional connectivity strength at each of four wavelet scales (corresponding to frequency intervals) and over all frequencies (broadband) for Sz (red), Rel (green), and HV (blue). Connectivity strength (wavelet correlation) was corrected for nonsignificant age differences between groups by regression. Red asterisks denote significant rank-ordered differences in connectivity strength: Sz < Rel < HV (J-T test, $P < 0.05$, FDR corrected). Crosses denote values located more than 1.5× the interquartile range from the median.

test the hypothesis that brain network randomization/resilience is an endophenotype, or marker of familial risk for schizophrenia, that is expected to be abnormal in nonpsychotic first-degree relatives of patients as well as in the patients themselves.

We therefore analyzed resting-state fMRI data from 25 patients with schizophrenia (Sz), 25 first-degree relatives (Rel), and 29 healthy volunteers (HV). For each individual image, we constructed a functional brain graph and estimated some key topological and geometric markers of randomization (clustering coefficient, efficiency, degree distribution, distance distribution), and resilience to targeted attack and random failure. We predicted that functional brain networks would be more randomized and resilient in both Sz and Rel, compared with HV.

Results

Functional Connectivity. At each frequency interval defined by a wavelet decomposition of the fMRI time series, the rank ordering of group mean functional connectivity HV > Rel > Sz was statistically significant [Jonckheere–Terpstra (J-T) test, $P < 0.05$, false discovery rate (FDR) corrected]. Post hoc t tests demonstrated that mean wavelet correlation, or functional connectivity, was significantly reduced in Sz compared with HV at all wavelet scales (Fig. 1). For consistency with many prior studies of resting-state fMRI connectivity, we focused on the frequency interval 0.05–0.1 Hz, approximately corresponding here to wavelet scale 2. However, we note that broadly similar results were obtained by analysis of other wavelet scales (Fig. S1).

Global Network Topology. There were significant between-group differences in all global topological metrics. For the clustering coefficient, the rank ordering HV > Rel > Sz was significant (J-T test; $P < 0.05$, FDR corrected; Fig. 2A), and post hoc t tests demonstrated significantly decreased clustering coefficient in people with schizophrenia, and their unaffected relatives, compared with healthy volunteers. In contrast, for the global efficiency, the rank ordering Sz > Rel > HV was statistically significant and post hoc t tests demonstrated significantly increased global efficiency in Sz, and Rel, compared with HV (Fig. 2B). Small worldness was generally evident over a range of graph connection densities—the

so-called small-world regime corresponding to 1–24% connection density. There were significant differences in small worldness between groups: HV > Rel > Sz; and post hoc t tests demonstrated significant reductions in Sz compared with HV; small worldness was not abnormal in Rel (Fig. 2C).

Degree Distributions. The best-fitting form of the degree distribution was generally an exponentially truncated power law. However, there were significant differences between groups in terms of mean degree distribution parameters over the small-world regime: rank ordering Sz = Rel > HV for the power law exponent, α (J-T test, uncorrected $P = 0.026$), but rank ordering HV > Rel = Sz for the exponential cutoff, β (J-T test, uncorrected $P = 0.029$). Post hoc t tests demonstrated that the power law exponent α was significantly increased but the exponential cutoff β was significantly reduced in Sz and/or Rel, compared with HV. As shown graphically in Fig. 2D, this shift in degree distribution parameters indicates that the probability of
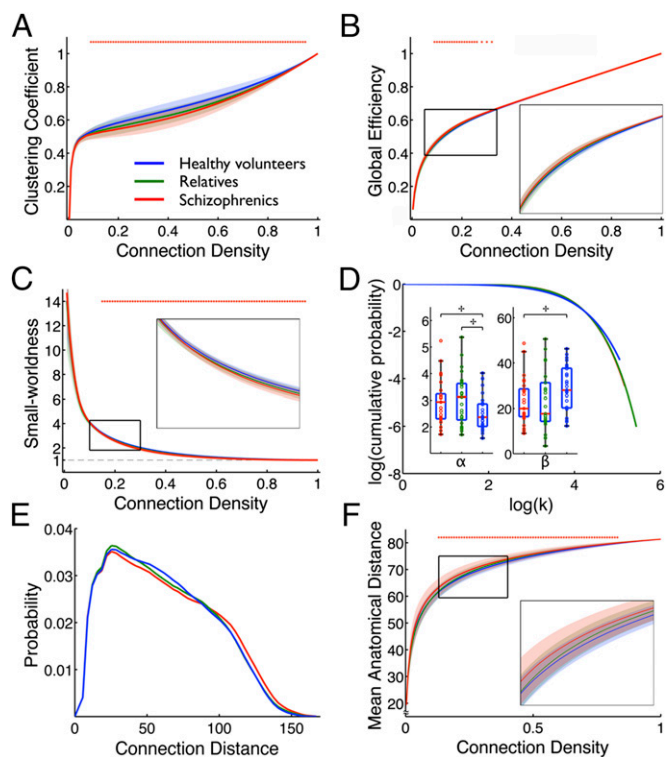

Fig. 2. Topological and geometric measures of functional brain networks in Sz (red), Rel (green), and HV (blue); confidence intervals on the curves represent ±1 SD. (A) Clustering coefficient (y axis) as a function of connection density (x axis). (B) Global efficiency (y axis) as a function of connection density (x axis). (C) Small worldness (y axis) as a function of connection density (x axis). (D) Cumulative degree distributions were best fit in each group by an exponentially truncated power law. The fitted curves with median value of the power law exponent α in each group are plotted; (Inset) boxplots represent the within-group distributions and between-group differences in the two parameters: α and the exponential cutoff, β; cross indicates significant between-group differences (t test, uncorrected $P < 0.05$). (E) The probability distributions of connection distance in three groups (data averaged over subjects in each group) show a greater proportion of long-distance connections, and reduced proportion of middistance connections, in schizophrenia. (F) The mean connection distance (x axis) as a function of connection density (y axis) shows a significant trend in rank ordering of the three groups, Sz > Rel = HV, where the network has longer connection distance in Sz, but not in Rel. The significant differences between groups are denoted by asterisks (J-T test, $P < 0.05$, FDR corrected).
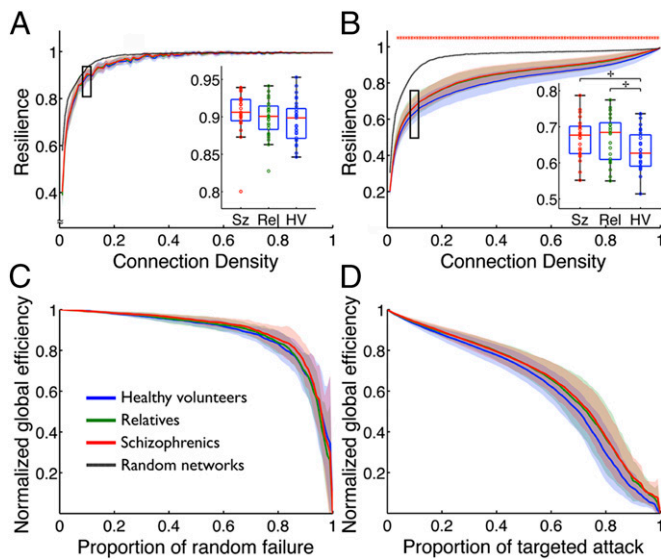
Fig. 3. Network resilience to target attack and random failure for Sz (red), Rel (green), and HV (blue); confidence intervals on the curves represent ±1 SD. (*A*) Network resilience against random failure (*y* axis) as a function of connection density (*x* axis). (*B*) Network resilience against targeted attack (*y* axis) as a function of connection density (*x* axis). The boxplots illustrate the network resilience at connection density of 10%; the significant differences between the three groups are denoted by red asterisks (J-T test, $P < 0.05$, FDR corrected); and cross denotes post hoc *t* tests with uncorrected $P < 0.05$. (*C* and *D*) The curves show how the global efficiency (percentage of maximum efficiency; *y* axis) of networks deteriorates as the proportion of nodes deleted by in silico attack (*x* axis) is increased, at connection density of 10%. (*C*) Random failure causes less rapid deterioration of global efficiency in all networks. (*D*) Targeted attack on network hubs causes relatively rapid deterioration in network efficiency. Sz and Rel have greater resilience to targeted attack than healthy volunteers.

high degree hubs is abnormally reduced in both people with schizophrenia and their relatives.

Connection Distance. The distribution of connection distance was somewhat similar in all groups (Kolmogorov–Smirnov test, pairwise comparison, $P > 0.05$) (Fig. 2*E*). However, the mean connection distance over a range of connection densities (1–24%) was different between groups: The rank ordering Sz > Rel = HV was significant (J-T test, $P < 0.05$, FDR corrected, Fig. 2*F*), and post hoc *t* tests demonstrated significantly longer connection distance in Sz than in HV (uncorrected $P < 0.05$).

Resilience. Under random failure, the global efficiency of the networks typically remained high (about 90% of maximum efficiency), even after more than 50% of nodes had been deleted. In other words, brain networks were highly resilient to random failure (Fig. 3 *A* and *C*). However, the global efficiency of all networks was degraded more severely by targeted attack (Fig. 3 *B* and *D*). For example, after deletion of only 10% of the highest-degree hub nodes, the global efficiency of brain networks was reduced below 90% of maximum (Fig. 3*D*). For random failure, there were no significant between-group differences (J-T test, $P > 0.05$, FDR corrected). However, for targeted attack, the rank order Sz = Rel > HV was significant (J-T test, $P < 0.05$, FDR corrected), and post hoc *t* tests demonstrated that resilience to targeted attack was increased in both Sz and Rel compared with HV (Fig. 3).

Nodal Topology. There were significant between-group differences in clustering and efficiency at a nodal level of analysis that were consistent with the results for global topology (J-T test, $P < 0.05$,

FDR corrected). As illustrated in Fig. 4*A*, for nodal clustering, the rank ordering was usually HV > Rel > Sz, whereas, for nodal efficiency, the rank ordering was usually Sz > Rel > HV. Nodes demonstrating significant rank ordering of clustering HV > Rel > Sz were located mainly in bilateral precentral and postcentral cortex, and lateral and medial occipital cortex. These are areas of functionally specialized cortex (motor, somatosensory, and visual) that are known to be highly clustered in healthy functional brain networks (16). Nodes demonstrating significant rank ordering of efficiency Sz > Rel > HV were localized in dorsolateral prefrontal cortex, anterior and posterior cingulate cortex, inferior parietal cortex, superior temporal cortex, hippocampus, and caudate nucleus. All of these areas have been previously implicated in the pathophysiology of schizophrenia (11).

Schizophrenia-related differences in nodal topology were also related to the nodal topology of the normal connectome. Specifically, the nodes that showed the greatest reduction of clustering in schizophrenia tended to have the highest clustering in the HV group ($r = -0.78$, $P < 0.001$), whereas nodes that showed the greatest increase of efficiency in schizophrenia tended to have the lowest efficiency in the HV groups ($r = -0.65$, $P < 0.001$) (Fig. 4*B*). Similar results were also found in Rel; see Figs. S2 and S3 and Tables S1 and S2.

Correlational Analysis of Network Metrics and Clinical Variables. The network metrics were moderately correlated with each other (Table S3). Over all participants in the study, connectivity strength was negatively correlated with physical (Euclidean) distance of functional connections ($r = -0.30$) and with three topological measures of network integration: global efficiency ($r = -0.40$), resilience to targeted attack ($r = -0.65$), and the
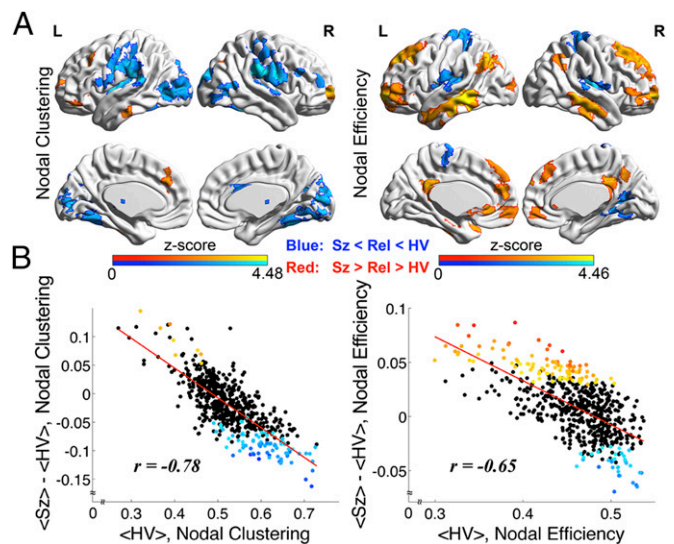

Fig. 4. Nodal topological differences between groups. (*A*) Cortical surface maps show significant between-group differences in rank order of nodal clustering (*Left*) and nodal efficiency (*Right*) of functional brain networks (J-T trend test, $P < 0.05$, FDR corrected). Nodes where the rank order is Sz < Rel < HV are colored in blue; nodes where the rank order is Sz > Rel > HV are colored in red. The cortical surface maps were generated by BrainNet viewer software (www.nitrc.org/projects/bnv/) (52). (*B*) The mean nodal topology in the HV group (*x* axis) versus the difference between HV and Sz groups in mean nodal topology (*y* axis) are plotted for nodal clustering (*Left*) and nodal efficiency (*Right*). The colored points highlight nodes demonstrating significant between-group differences in nodal topology corresponding to the colored areas of the cortical surface maps (*A*). The straight lines fitted to these data have significantly nonzero negative slope, indicating that abnormally increased efficiency tends to be located in nodes with normally low efficiency whereas abnormally decreased clustering is located in nodes with normally high clustering.

NEUROSCIENCE

power law exponent of a truncated power law degree distribution ($r = -0.58$). In other words, low strength connections tended to traverse long distances and to be important for both (*i*) the emergence of high-degree hubs, conferring vulnerability to targeted attack, and (*ii*) short characteristic path length or high global efficiency. On the other hand, connectivity strength was positively correlated with clustering coefficient ($r = 0.69$) and the exponential cutoff parameter of the degree distribution ($r = 0.56$), meaning that high strength connections tended to be important both for a more homogeneous degree distribution and for more clustered or segregated topology. Repeating this correlational analysis group by group, we found that the same relationships between connectivity strength, resilience, and power law degree distribution parameter were consistently and significantly expressed in each group. The relationship between strength and distance was not significant in any individual group, which may reflect the fact that functional connectivity strength decays as a nonlinear function of distance and correlation is a measure of linear association (16). The normal relationship between strength and global efficiency was not expressed by Sz or Rel; see Table S3 for details.

In the Sz group only, we explored the relationships between all network metrics and questionnaire measures of psychotic symptom severity [the Positive and Negative Syndrome Scale (PANSS) global and subscale scores] and a measure of current antipsychotic drug exposure (chlorpromazine equivalent dose, milligrams per day). The global psychotic symptom score was negatively correlated with connection distance ($r = -0.47$); there were no other significant associations between clinical variables and network measures. Antipsychotic drug exposure was negatively correlated with both global efficiency ($r = -0.53$) and small worldness ($r = -0.64$), but these effects were not significant after exclusion of a single outlier with very high antipsychotic drug exposure; see Table S3 and Fig. S4 for details.

Discussion

It is encouraging that many of these graph theoretical results on an independent Chinese sample are consistent with prior functional network studies of schizophrenia in US or European populations, suggesting that these are internationally replicable diagnostic markers. The global and nodal topological changes of increased global efficiency and decreased clustering coefficient are consistent with prior reports of "subtle randomization" of brain networks in schizophrenia (5–8). Randomization is also consistent with the degree distribution being less fat tailed, and the distance distribution being more weighted toward long-distance connections, in schizophrenia (6).

In this context, it is empirically more novel, although conceptually not surprising, that schizophrenia should also be associated with greater than normal resilience of functional networks to targeted attack. Random graphs, as shown in Fig. 3, maintain high levels of global efficiency even after a large percentage of nodes have been deleted, whether randomly or by targeted attack on the higher-degree hubs. Complex networks, like the brain, the Internet, and many other nonrandom systems, are more vulnerable to targeted attack because they have more heterogeneous degree distributions than a random graph, and the deletion of high-degree hubs consequently has a more serious effect on the global integrity of the network (17). Thus, it is predictable that functional networks in schizophrenia, being topologically more random than normal, and with a less heterogeneous degree distribution, should be more resilient to targeted attack, as we have shown.

We interpret this result by supposing that topological resilience may be advantageous, to some extent, simply because it protects the integrity of the network from pathological attack. It seems increasingly clear from neuroimaging studies of brain network topology in neurological and psychiatric disorders that "lesions" of gray matter measured by MRI tend to be concentrated in high-degree hub regions of the brain (18, 19). This pattern of results is compatible with the hypothesis that hubs are preferentially vulnerable to pathogenesis and/or that damaged hubs are especially likely to be symptomatic. There is also evidence from pathogenic modeling of neurodegenerative processes on imaging networks that Alzheimer's disease and related disorders can be understood to progress by propagation between nodes, which will naturally expose the hubs of the brain to the degenerative process at a relatively early stage in its propagation through the connectome (20, 21).

Given this prior evidence that brain disorders preferentially target high-degree hub nodes, it seems reasonable to expect that brain networks with greater resilience to computational attack on their hubs might in real life confer some survival advantage in the face of pathological attack. This advantage might exert a positive selection pressure on genes favoring network randomization, which might in turn explain the persistence in the population of alleles that, at "high dose" or in adverse combinations, are associated with increased incidence of a disabling neurodevelopmental disorder like schizophrenia. However, it is possible that there is some other factor that drives emergence of this systems-level endophenotype, and its hypothetically greater resilience to pathological attack is immaterial to its selection. One testable hypothesis generated by these reflections is that the first-degree relatives of patients with schizophrenia might have reduced incidence or severity of brain disorders, such as Alzheimer's disease, that are associated with gray matter volume deficits in structural network hubs.

A conceptually related previously unidentified result of this study is that it is the first, to our knowledge, to demonstrate that topological abnormalities of functional networks are also evident in the nonpsychotic, first-degree relatives of patients. Compared with HV, we have shown that Rel had significantly reduced clustering coefficient, increased efficiency, less fat-tailed degree distributions, and greater resilience to targeted attack. In other words, fMRI networks in Rel also demonstrated an abnormal shift to greater randomization of network topology. These results suggest that fMRI network randomization is a marker of genetic or shared environmental risk for disorder, rather than simply a marker of schizophrenia per se. Equally, the abnormal topological profile in the fMRI networks of Rel discounts possible interpretations of the abnormalities in the Sz group in terms of their exposure to antipsychotic medication or other factors specifically related to a clinical diagnosis of schizophrenia. Given the high heritability of functional connectivity and functional network markers (22, 23), and the high heritability of schizophrenia, it is plausible that the abnormalities of network randomization demonstrated here represent the effects of genetic variants conferring risk for schizophrenia. However, it would require a twin study to rule out the alternative possible interpretation that network randomization is indicative of shared environmental effects.

Two questions in particular arise when thinking about these putative network endophenotypes of schizophrenia. First, what is different about the network configuration of patients compared with their relatives that could explain why the relatives are not psychotic? We do not have a complete answer to this question, but it is notable that Rel did not converge in all respects on the pattern of network abnormalities described in Sz. For example, Sz had significantly reduced small worldness, and greater proportion of long-distance connections, whereas Rel were not significantly different from normal on these measures. On many other topological measures (such as efficiency and resilience to targeted attack), it was also notable that the average scores of Rel were intermediate between the scores of Sz and HV. In short, the randomization endophenotype may be more topologically extreme and/or more biologically expensive in patients compared with their first-degree relatives.

A second key question concerns the potentially beneficial aspects of network randomization. It has been shown that higher-IQ

individuals tend to have more-efficient structural and functional networks (24, 25), that more-difficult cognitive tasks demand more-integrated or efficient functional network topology (26, 27), and that a pharmacological challenge (acute nicotine replacement in abstinent cigarette smokers) that enhanced attention also increased efficiency and connection distance of fMRI networks (28). These observations are consistent with earlier theoretical claims that higher-order conscious processing depends on access to a "global workspace" rather than a segregated, modular architecture (29–31). This would imply that the greater efficiency of more random network organization in patients with schizophrenia should be associated with superior performance on higher-order cognitive tasks. However, in fact, this is not the case for schizophrenia, which is typically associated with moderate to severe impairments in executive function and working memory. The normal link between greater network efficiency and superior cognitive performance seems to be disrupted in schizophrenia, for reasons that are not yet known.

There are several limitations to this work. Sz were receiving antipsychotic drugs that can affect functional connectivity and network topology (32, 33). However, this cannot explain the network abnormalities in Rel, as they were unmedicated (except one who was taking antidepressants). A more fundamental limitation is that the edges of fMRI networks represent above-threshold correlations between time series, but the underlying biological substrate of this functional connectivity is not well characterized. We used Euclidean distance between nodes as a simple measure of the physical distance of edges in the functional brain graphs. Because functional connectivity does not securely imply a direct anatomical connection (34), and because anatomical connections are typically not linear, the Euclidean distance will generally be an underestimate of the true anatomical (axonal) distance between functionally connected areas of the brain. We have assumed that this bias applies consistently between groups and therefore does not substantively distort the rank order of different groups in terms of connection distance. Developments in human diffusion-weighted imaging may provide more-accurate estimates of the anatomical connection distance subtending functional connectivity in future. The construction of brain graphs from any modality of neuroimaging data entails multiple methodological choices about preprocessing and analysis that could influence the pattern of results. We have addressed this issue by testing that key results are robust to contemporary standards for correction of head motion (35–37) and to reasonable variation in other analysis steps, including choice of parcellation, wavelet scale, and connection density.

Methods

Sample. We recruited three groups of participants: patients with schizophrenia, Sz ($n = 35$); the first-degree relatives of patients with schizophrenia, Rel ($n = 39$); and healthy volunteers, HV ($n = 36$). Sz and Rel were recruited from the Psychiatric Outpatient Department of Lo-Sheng Sanatorium and Hospital in Taipei, Taiwan. Sz were diagnosed according to the *Diagnostic and Statistical Manual of Mental Disorders-IV* criteria (38) for schizophrenia, and completed PANSS (39) for evaluation of psychotic symptom severity. Rel and HV were cognitively normal with no history of neurological or psychiatric disorders, and had no cognitive complaints, confirmed by Mini-International Neuropsychiatric Interview (40). After elimination of subjects due to uncontrolled head motion and to optimize matching of the remaining groups for age and sex, the final sample included 25 Sz, 25 Rel, and 29 HV subjects; see *SI Text*, Table S4, and Fig. S5 for details. There were no significant differences between groups in terms of sex, age, handedness (41), or mean or maximum head displacement. All Sz were medicated: 9 Sz were taking typical antipsychotics, of which 2 were also taking antidepressants; 14 Sz were taking atypical antipsychotics, of which 2 were also taking antidepressants; and 2 Sz were taking antidepressants only. The average antipsychotic dose was 408 mg/d in chlorpromazine equivalents. One Rel had a history of mild depressive disorder and was taking antidepressants. The remaining participants were not taking any medication at the time of study. The study was approved by the Institutional Review Board of Taichung

Veterans General Hospital, Taichung, Taiwan. All participants gave informed consent in writing. Further details on sample recruitment and assessment are provided in *SI Text*.

Magnetic Resonance Imaging. Resting-state fMRI data were acquired using a 3T MR system (Siemens Magnetom Tim Trio) at National Yang-Ming University, Taipei, Taiwan, using a gradient echo-planar imaging sequence sensitive to blood oxygenation level-dependent contrast; see *SI Text* for detailed imaging protocols.

fMRI Preprocessing. The preprocessing procedures for the fMRI datasets in native space included slice-timing correction; motion correction to the first volume with rigid-body alignment; obliquity transform to the structural MR image; spatial smoothing within functional mask with a 6-mm at full-width at half-maximum Gaussian kernel; intensity normalization to a whole brain median of 1,000 (35, 37); wavelet despike (removing signal transients related to small amplitude (<1 mm) head movements) (37); and multiple regression of motion parameters and their first derivatives, and the global average white matter (WM) and cerebrospinal fluid (CSF) signals, from the fMRI time series data. The effects of transient micromovements on functional connectivity were carefully assessed and controlled in individuals and groups; see refs. 35–37 and *SI Text*. Preprocessed data were spatially normalized to Montreal Neurological Institute (MNI) stereotactic standard space by an affine transformation and interpolated to 3.4-mm cubic voxels. The gray matter areas were parcellated into 638 regions of approximately similar size (26), and gray matter regions were excluded if the signal quality in regions was not satisfactory in all participants, resulting in a set of 585 motion-corrected, regional mean fMRI time series for each participant; see *SI Text* and Fig. S6 for details. Preprocessing, spatial normalization, and parcellation procedures were implemented with Analysis of Functional NeuroImages (AFNI) (42) and FMRIB Software Library (FSL v5.02, fsl.fmrib.ox.ac.uk/fsl/fslwiki/). The BrainWavelet Toolbox was used for correction of transient head movements (37) (www.brainwavelet.org).

Functional Connectivity Estimation. We used the maximal overlap discrete wavelet transform with a Daubechies 4 wavelet to decompose each fMRI time series into four scales or frequency intervals: scale 1, 0.10–0.20 Hz; scale 2, 0.05–0.10 Hz; scale 3, 0.025–0.05 Hz; and scale 4, 0.0125–0.025 Hz. We estimated the pairwise wavelet correlations between the wavelet coefficients at each scale for each of 183,921 possible pairs of regions.

Graph Theoretical Analysis of Network Connections. The absolute wavelet correlation matrices were used to construct binary undirected graphs. The minimum spanning tree that connected all 585 regional nodes with 584 edges was first defined, and then additional edges were added in decreasing order of wavelet correlation to construct a series of graphs for each individual with connection density in the range 1–100% in increments of 1% (5, 6). The following global topological parameters were estimated for each graph at each connection density: global efficiency, a measure of network integration; clustering coefficient, a measure of network segregation; and small worldness, the ratio of normalized clustering to normalized efficiency. The degree, clustering, and efficiency were also estimated for each regional node. All of these metrics have been frequently used in prior graph theoretical studies of fMRI data (43–47) and are described in more detail in *SI Text*. They were estimated using MATLAB code in the Brain Connectivity Toolbox (see ref. 47; www.brain-connectivity-toolbox.net).

Degree Distribution, Network Connection Distance, and Resilience. The probability distribution of degree (K) over all nodes in the network (the degree distribution) was best fit to an exponentially truncated power law $P(K) = K^{\alpha-1}e^{K/\beta}$, which has two parameters, the power law exponent, α, and the exponential cutoff, β (16); see *SI Text* for details. The connection distance was simply defined as the Euclidean distance between the centroids of each pair of regional nodes connected by an edge in MNI stereotactic standard space (6, 16). To test the resilience of each network, we simulated attacks on the network by removal of nodes either in descending order of their degree (targeted attack on hubs) or in random order (random failure). We thus incrementally increased the percentage of deleted nodes from 0 to 100% in increments of 1%, and recalculated the global efficiency of the remaining network after deletion of each node (17). The area under the curve of normalized global efficiency (scaled to maximum) versus the percentage of deleted nodes was defined as a summary measure of the resilience of a network (48).

Nodal Topology. Efficiency and clustering were estimated for each regional node in the series of networks with connection density in the range 1–24%, in increments of 1%. To explore the relationship between abnormal nodal topology in patients and normative nodal topology, the difference of nodal topology between Sz and HV groups at each node was correlated with the corresponding nodal topology metric in the HV group only (49).

Statistical Analysis and Hypothesis Testing. To assess the ordered between-group differences in the measures of functional connectivity and functional network organization, we used the J-T test (50) to test the hypotheses that metrics were ranked in the order Sz > Rel > HV or HV > Rel > Sz. If this test indicated significant differences between the medians of all three groups, we conducted additional pairwise t tests to compare network metrics between Sz versus HV groups and Rel versus HV groups. Two significance levels of stringency were set for statistical testing: uncorrected $P < 0.05$ and FDR correction at the 5% level (51).

1. Stephan KE, Friston KJ, Frith CD (2009) Dysconnection in schizophrenia: From abnormal synaptic plasticity to failures of self-monitoring. *Schizophr Bull* 35(3):509–527.
2. Friston KJ, Frith CD (1995) Schizophrenia: A disconnection syndrome? *Clin Neurosci* 3(2):89–97.
3. Volkow ND, et al. (1988) Brain interactions in chronic schizophrenics under resting and activation conditions. *Schizophr Res* 1(1):47–53.
4. Bullmore ET, Frangou S, Murray RM (1997) The dysplastic net hypothesis: An integration of developmental and dysconnectivity theories of schizophrenia. *Schizophr Res* 28(2-3):143–156.
5. Alexander-Bloch AF, et al. (2010) Disrupted modularity and local connectivity of brain functional networks in childhood-onset schizophrenia. *Front Syst Neurosci* 4:147.
6. Alexander-Bloch AF, et al. (2013) The anatomical distance of functional connections predicts brain network topology in health and schizophrenia. *Cereb Cortex* 23(1):127–138.
7. Liu Y, et al. (2008) Disrupted small-world networks in schizophrenia. *Brain* 131(Pt 4):945–961.
8. Lynall ME, et al. (2010) Functional connectivity and brain networks in schizophrenia. *J Neurosci* 30(28):9477–9487.
9. Rubinov M, et al. (2009) Small-world properties of nonlinear brain activity in schizophrenia. *Hum Brain Mapp* 30(2):403–416.
10. van den Heuvel MP, Mandl RC, Stam CJ, Kahn RS, Hulshoff Pol HE (2010) Aberrant frontal and temporal complex network structure in schizophrenia: A graph theoretical analysis. *J Neurosci* 30(47):15915–15926.
11. Fornito A, Zalesky A, Pantelis C, Bullmore ET (2012) Schizophrenia, neuroimaging and connectomics. *Neuroimage* 62(4):2296–2314.
12. Wang Q, et al. (2012) Anatomical insights into disrupted small-world networks in schizophrenia. *Neuroimage* 59(2):1085–1093.
13. Stam CJ, Reijneveld JC (2007) Graph theoretical analysis of complex networks in the brain. *Nonlinear Biomed Phys* 1(1):3.
14. van den Heuvel MP, et al. (2013) Abnormal rich club organization and functional brain dynamics in schizophrenia. *JAMA Psychiatry* 70(8):783–792.
15. Bassett DS, et al. (2008) Hierarchical organization of human cortical networks in health and schizophrenia. *J Neurosci* 28(37):9239–9248.
16. Achard S, Salvador R, Whitcher B, Suckling J, Bullmore E (2006) A resilient, low-frequency, small-world human brain functional network with highly connected association cortical hubs. *J Neurosci* 26(1):63–72.
17. Albert R, Jeong H, Barabasi AL (2000) Error and attack tolerance of complex networks. *Nature* 406(6794):378–382.
18. Crossley NA, et al. (2014) The hubs of the human connectome are generally implicated in the anatomy of brain disorders. *Brain* 137(Pt 8):2382–2395.
19. Bullmore E, Sporns O (2012) The economy of brain network organization. *Nat Rev Neurosci* 13(5):336–349.
20. Seeley WW, Crawford RK, Zhou J, Miller BL, Greicius MD (2009) Neurodegenerative diseases target large-scale human brain networks. *Neuron* 62(1):42–52.
21. Raj A, Kuceyeski A, Weiner M (2012) A network diffusion model of disease progression in dementia. *Neuron* 73(6):1204–1215.
22. Fornito A, Bullmore ET (2012) Connectomic intermediate phenotypes for psychiatric disorders. *Front Psychiatry* 3:32.
23. van den Heuvel MP, et al. (2013) Genetic control of functional brain network efficiency in children. *Eur Neuropsychopharmacol* 23(1):19–23.
24. van den Heuvel MP, Stam CJ, Kahn RS, Hulshoff Pol HE (2009) Efficiency of functional brain networks and intellectual performance. *J Neurosci* 29(23):7619–7624.
25. Li Y, et al. (2009) Brain anatomical network and intelligence. *PLOS Comput Biol* 5(5):e1000395.
26. Crossley NA, et al. (2013) Cognitive relevance of the community structure of the human brain functional coactivation network. *Proc Natl Acad Sci USA* 110(28):11583–11588.
27. Kitzbichler MG, Henson RN, Smith ML, Nathan PJ, Bullmore ET (2011) Cognitive effort drives workspace configuration of human brain functional networks. *J Neurosci* 31(22):8259–8270.
28. Giessing C, Thiel CM, Alexander-Bloch AF, Patel AX, Bullmore ET (2013) Human brain functional network changes associated with enhanced and impaired attentional task performance. *J Neurosci* 33(14):5903–5914.
29. Baars BJ (1993) *A Cognitive Theory of Consciousness* (Cambridge Univ Press, Cambridge, UK).
30. Dehaene S, Naccache L (2001) Towards a cognitive neuroscience of consciousness: Basic evidence and a workspace framework. *Cognition* 79(1-2):1–37.
31. Fodor JA (1983) *The Modularity of Mind* (MIT Press, Cambridge, MA).
32. Bolding MS, et al. (2012) Antipsychotic drugs alter functional connectivity between the medial frontal cortex, hippocampus, and nucleus accumbens as measured by H215O PET. *Front Psychiatry* 3:105.
33. Lui S, et al. (2010) Short-term effects of antipsychotic treatment on cerebral function in drug-naive first-episode schizophrenia revealed by "resting state" functional magnetic resonance imaging. *Arch Gen Psychiatry* 67(8):783–792.
34. Honey CJ, et al. (2009) Predicting human resting-state functional connectivity from structural connectivity. *Proc Natl Acad Sci USA* 106(6):2035–2040.
35. Power JD, Barnes KA, Snyder AZ, Schlaggar BL, Petersen SE (2012) Spurious but systematic correlations in functional connectivity MRI networks arise from subject motion. *Neuroimage* 59(3):2142–2154.
36. Satterthwaite TD, et al. (2012) Impact of in-scanner head motion on multiple measures of functional connectivity: Relevance for studies of neurodevelopment in youth. *Neuroimage* 60(1):623–632.
37. Patel AX, et al. (2014) A wavelet method for modeling and despiking motion artifacts from resting-state fMRI time series. *Neuroimage* 95:287–304.
38. American Psychiatric Association (1994) *Diagnostic and Statistical Manual of Mental Disorders* (Am Psychiatr Assoc, Washington, DC), 4th Ed.
39. Kay SR, Fiszbein A, Opler LA (1987) The Positive and Negative Syndrome Scale (PANSS) for schizophrenia. *Schizophr Bull* 13(2):261–276.
40. Sheehan DV, et al. (1998) The Mini-International Neuropsychiatric Interview (M.I.N.I.): The development and validation of a structured diagnostic psychiatric interview for DSM-IV and ICD-10. *J Clin Psychiatry* 59(Suppl 20):22–33, quiz 34–57.
41. Oldfield RC (1971) The assessment and analysis of handedness: The Edinburgh inventory. *Neuropsychologia* 9(1):97–113.
42. Cox RW (1996) AFNI: Software for analysis and visualization of functional magnetic resonance neuroimages. *Comput Biomed Res* 29(3):162–173.
43. Bassett DS, Bullmore ET (2009) Human brain networks in health and disease. *Curr Opin Neurol* 22(4):340–347.
44. He Y, Evans A (2010) Graph theoretical modeling of brain connectivity. *Curr Opin Neurol* 23(4):341–350.
45. Bullmore E, Sporns O (2009) Complex brain networks: Graph theoretical analysis of structural and functional systems. *Nat Rev Neurosci* 10(3):186–198.
46. Boccaletti S, Latora V, Moreno Y, Chavez M, Hwang DU (2006) Complex networks: Structure and dynamics. *Phys Rep* 424(4-5):175–308.
47. Rubinov M, Sporns O (2010) Complex network measures of brain connectivity: Uses and interpretations. *Neuroimage* 52(3):1059–1069.
48. van den Heuvel MP, Sporns O (2011) Rich-club organization of the human connectome. *J Neurosci* 31(44):15775–15786.
49. Achard S, et al. (2012) Hubs of brain functional networks are radically reorganized in comatose patients. *Proc Natl Acad Sci USA* 109(50):20608–20613.
50. Bewick V, Cheek L, Ball J (2004) Statistics review 10: Further nonparametric methods. *Crit Care* 8(3):196–199.
51. Genovese CR, Lazar NA, Nichols T (2002) Thresholding of statistical maps in functional neuroimaging using the false discovery rate. *Neuroimage* 15(4):870–878.
52. Xia M, Wang J, He Y (2013) BrainNet Viewer: A network visualization tool for human connectomics. *PLoS ONE* 8(7):e68910.
53. Heaton RK (1981) *A Manual for the Wisconsin Card Sorting Test* (Psychological Assessment Resources, Odessa, FL).
54. Tzourio-Mazoyer N, et al. (2002) Automated anatomical labeling of activations in SPM using a macroscopic anatomical parcellation of the MNI MRI single-subject brain. *Neuroimage* 15(1):273–289.
55. Zalesky A, et al. (2010) Whole-brain anatomical networks: Does the choice of nodes matter? *Neuroimage* 50(3):970–983.
56. Triantafyllou C, et al. (2005) Comparison of physiological noise at 1.5 T, 3 T and 7 T and optimization of fMRI acquisition parameters. *Neuroimage* 26(1):243–250.
57. Molloy EK, Meyerand ME, Birn RM (2014) The influence of spatial resolution and smoothing on the detectability of resting-state and task fMRI. *Neuroimage* 86:221–230.
58. Watts DJ, Strogatz SH (1998) Collective dynamics of 'small-world' networks. *Nature* 393(6684):440–442.
59. Latora V, Marchiori M (2001) Efficient behavior of small-world networks. *Phys Rev Lett* 87(19):198701.
60. Humphries MD, Gurney K, Prescott TJ (2006) The brainstem reticular formation is a small-world, not scale-free, network. *Proc Biol Sci* 273(1585):503–511.
61. Achard S, Bullmore E (2007) Efficiency and cost of economical brain functional networks. *PLOS Comput Biol* 3(2):e17.